

Peculiarities of mitochondrial chloride channel kinetics

Anton Misak¹ and Zuzana Sevcikova Tomaskova² 

¹ *Institute of Clinical and Translational Research, Biomedical Research Center, v.v.i., Slovak Academy of Sciences, Bratislava, Slovakia*

² *Institute of Molecular Physiology and Genetics, Centre of Biosciences, v.v.i., Slovak Academy of Sciences, Bratislava, Slovakia*

Abstract. Cardiac mitochondrial chloride channels are involved in the regulation of mitochondrial membrane potential, with impact on the sarcolemma action potential. Despite their importance, they still lack molecular identity. So far, the most probable hypothesis is that they are part of the CLIC channel family. Here, we report a detailed profile of these channels under different conditions. We find this characterization essential for their identification and comparison with other chloride channels. The presence of many unresolved closed events at higher acquisition rate and extremely long closings were detected, which was consistent with the power-law distribution. On the other hand, the channel openings were described by a single-exponential function. We compare the results with ion channels of similar dwell time distribution and discuss the possible connections to other chloride channels and channel families, including the CLIC family. Moreover, the described kinetic features call for theoretical interpretation and proper single-channel analysis.

Key words: Cardiac mitochondria — Chloride channel — Gating kinetics — Markov process — Dwell time distribution

Introduction

The chloride channels present in the inner mitochondrial membrane are involved in the regulation of mitochondrial membrane potential. While their role under oxidative stress has been suggested by multiple complex studies on whole cardiomyocytes (Aon et al. 2003; Cortassa et al. 2004; Aon et al. 2009), the molecular identity of these channels remains uncertain. It has been shown recently that chloride intracellular channels (CLIC) are localized in the mitochondrial membrane (Ponnalagu et al. 2016). The activity measured from isolated mitochondrial membranes has not been connected to any CLIC protein isoform yet, though the chloride channels from native mitochondrial membrane are strong

candidates for CLIC (Ponnalagu et al. 2016; Tomasek et al. 2017). So far, this statement is without direct evidence.

In general, each ion channel protein has characteristic changes in conformation, some of which lead to the opening of the conductive pore (Sansom 1995; Doyle 2004; Reeves et al. 2008; Sakmann and Neher 2009; Flood et al. 2019). These changes, reflected by a set of dwell times (for open or closed state separately), are called gating kinetics. The movement of the transmembrane helices is often behind the gating process and, depending on the channel type, their tilting, rotation or bending has been observed (Doyle 2004). Moreover, the molecular dynamics simulations show a presence of intermediate states, through which a stable (with lower energy) conformation can be achieved (Flood et al. 2019). However, these intermediate states are not detectable by single-channel current measurements. Fitting of the dwell time histograms with a set of exponential functions has been the commonly applied method to determine the rate constants describing the distribution of dwell times. The underlying model is based on the assumption that the channel protein has a small discrete number of conformational states. The transitions

Electronic supplementary material. The online version of this article (doi: 10.4149/gpb_2022001) contains Supplementary material.

Correspondence to: Zuzana Sevcikova Tomaskova, Institute of Molecular Physiology and Genetics, Centre of Biosciences, v.v.i., Slovak Academy of Sciences, Bratislava, Slovakia
E-mail: zuzana.tomaskova@savba.sk

between these states are random (e.g. Markov process) and are described by kinetic rate constants (Hille 1992; Sakmann and Neher 2009).

However, these assumptions may not always be valid. In such cases the interpretation of the rate constants and the determination of the number of conformational states is not the appropriate approach. A method has been developed that does not require strong assumptions concerning the conformational changes of a channel (Liebovitch et al. 1987). This methodological approach was inspired by the fractal theory and thus was named “fractal analysis” of channel kinetics. The method uses histograms of dwell times with an increasing bin width. From a set of these histograms, the probability density function and “effective” rate constants can be calculated. It discerns different types of distribution – apart from exponential, also “stretch exponential” and power-law. The Markov model can only be applied in case of exponential distribution. The advantage of this approach is that one can prevent errors in determination (and interpretation) of rate constants and number of conformational states caused by inappropriate assumptions. The set of rate constants is given by the structure of the protein; therefore, it can be used as an “identification card” of this protein. The Markov model is based on the assumption that the channel gating involves transitions among a small number of discrete states and that the probability of leaving a kinetic state is independent of the time the state has been occupied (Wonderlin et al. 1990). On the contrary, the “fractal” model assumes that numerous conformational states are separated by small energy barriers, which is based on the dynamic motion of proteins. The second assumption is that the probability of leaving a state is dependent on the time the state had been occupied. Nevertheless, the method of fractal analysis is not generally accepted in the single channel current analysis, as several objections have been raised against it (Sakmann and Neher 2009).

Läuger concluded that for many channels the distribution of the open dwell times is simpler than the distribution of closed dwell times. The distribution of the closed dwell times often has a higher occurrence of longer dwell times that could not be described by an exponential function (Läuger 1988). A combined approach has been suggested by French and Stockbridge (1988), nevertheless, it has not been widely used. Of course, many channels do have the exponential dwell time distributions and it is not necessary to abandon the Markov model in such cases (Wonderlin et al. 1990). However, there are exceptions when the use of other than exponential fit of dwell time histograms might be considered (Millhauser et al. 1988).

Rotation, Brownian motions or atomic collisions occur in a protein at scale from femtoseconds to nanoseconds. These motions are faster than the transition of ions through channel pore. They can happen many times during a larger

conformational change of a protein, which reflects the change between conducting and non-conducting states (Hille 1992). The gating of an ion channel is much slower than the motion that takes place in the protein, where the gating typically occurs on a time scale of microseconds and seconds (Flood et al. 2019). The resolution of gating events from the single-channel recording is given by the acquisition rate and signal-to-noise ratio. When the signal is sampled at 4 kHz, the events shorter than twice the sampling period ($t_{\text{event}} < 500$ ms) are not properly detected and analyzed.

We analyzed the mitochondrial chloride channel gating kinetics, in particular its concentration and voltage dependence. Curiously, when visualized as a square root of the number of events *versus* the logarithm of time (“ \sqrt{N} vs. $\log t$ ”), the distribution of the closed dwell times did not exhibit a peak, but looked rather like an exponential decay, which was unusual. According to the commonly used concept the peak(s) should reflect the presence of characteristic dwell time(s), describable by exponential function(s). Moreover, the observation of many unresolved events even at a 5-fold higher acquisition rate (from 4 to 20 kHz) and the presence of long-lasting closures bursts (Tomaskova et al. 2007; Tomasek et al. 2017) inspired us to use a different type of kinetic analysis. The bursts of channel activity are described for many channels (Venglarik et al. 1993; Mienville and Clay 1996; Moss and Magleby 2001). However, the characteristic time for burst duration should be visible in “ \sqrt{N} vs. $\log t$ ” histogram (Wright et al. 1996; Sorum et al. 2017), which was not the case for the mitochondrial chloride channels. Instead, we used histograms with increasing bin width (Liebovitch et al. 1987, 2001; French and Stockbridge 1988) to describe the gating kinetics of mitochondrial chloride channels derived from rat heart. This “fractal analysis” approach is declared as suitable for determination of dwell time distribution pattern – to discern between power-law and exponential distribution.

We found that the closed dwell times had an obvious power-law distribution, while the distribution of the open dwell times was of a typical single-exponential character. The spectrum of the effective rate constants for leaving the closed state was almost invariant under all tested conditions. The changes in channel activity due to voltage or KCl concentration were reflected in the value of effective rate constants for leaving the open state.

Materials and Methods

Chemicals

Lipids were purchased from Avanti Polar Lipids (Alabaster, AL, USA). All chemicals were purchased from Sigma-Aldrich Chemie GmbH (Steinheim, Germany).

Isolation of mitochondrial membrane vesicles

Mitochondria from the hearts of male Wistar rats were isolated as described in detail in our previous study (Misak et al. 2013). The study was conducted according to the guidelines of the Directive 2010/63/EU of the European Parliament and approved by the Ethics Committee of Centre of Biosciences, Slovak Academy of Sciences and by the State Veterinary and Food Administration of the Slovak Republic (under numbers: Ro1715/11-221 and Ro3123/17-221). Shortly, the hearts were excised after thoracotomy. The ventricles were separated and homogenized. The homogenized tissue suspension was processed in several steps of differential centrifugation. Crude mitochondrial fraction was exposed to trypsin in order to disrupt tethers between sarcoplasmic reticulum and mitochondria. Immediately after trypsinization, a cocktail of protease inhibitors was added to the isolation buffer. The mitochondria were purified on Percoll density gradient, then washed and further processed by differential centrifugation and sonication, until the final fraction of submitochondrial particles was obtained. The membrane fraction was exposed to sonication at 35 kHz. The details of the isolation process and the purity of the obtained fraction was described in Misak et al. (2013). The final membrane fraction consisted mostly of outer and inner mitochondrial membranes. The membrane fraction was aliquoted and stored at -80°C until use. All procedures were performed at 4°C and isolation buffers contained a mixture of protease inhibitors. Two hearts were used in one isolation process. Overall, we recorded ion channels from two different isolations with data proportion 25% and 75%.

Single-channel current measurement

The native vesicles were fused into artificial bilayer lipid membrane (BLM) formed across an aperture (diameter approx. 0.1 mm) separating the *cis* and *trans* chamber. The composition of the solutions was: *trans*: 50 mM KCl, 2 mM MgCl_2 , 0.1 mM CaCl_2 , 0.3 mM EGTA, 10 mM HEPES, 5 mM Tris, pH 7.4, and *cis*: 0.25, 0.5, 0.75, 1, 1.5 or 2 M KCl, 2 mM MgCl_2 , 0.1 mM CaCl_2 , 0.3 mM EGTA, 10 mM HEPES, 5 mM Tris, pH 7.4. The single-channel current was measured by the bilayer clamp amplifier (BC-525C, Warner Instrument, Hamden, CT, USA) with sampling frequency 4 kHz, filtered with low-pass filter with 1 kHz cut-off frequency. For high resolution recording, the current was measured with sampling frequency 20 kHz and filtered with 5 kHz low-pass filter. The data were analyzed by Clampfit software (pClamp 9, Axon Instrument, USA). The *cis* side was grounded; under these experimental conditions, the positive current amplitude that increased upon the application of positive voltages corresponds to

the flux of chloride anions from the *cis* to the *trans* side. All procedures were carried out at room temperature ($22 \pm 1^{\circ}\text{C}$). The activity of the channels was quantified by open probability (P_{open}). P_{open} determined from N channels is expressed as median and interquartile range (Q_1 – Q_3). One-way ANOVA, followed by multiple comparison test was used to determine statistical significance (for slope values). Non-parametric Kruskal-Wallis test was used for comparison of $k_{\text{eff}}(1)$; the values of $k_{\text{eff}}(1)$ from individual experiments are expressed as median and interquartile range (Q_1 – Q_3). Table 1 summarizes the number of experiments under all tested conditions, along with the number of analyzed events (from pooled data).

Analysis of kinetics

The values of open and closed dwell times were exported from each current recording by Clampfit software. The software for analysis was prepared in Matlab (R2015a, <https://www.mathworks.com>; The MathWorks, Inc., USA).

The analysis was done according to Liebovitch et al. (1987) and Liebovitch and Sullivan (1987). We created a set of histograms by plotting the number of dwell times $N_i^{(n)}$ lying in the time interval $(t_i, t_i + \Delta t^{(n)})$, where i is the index of a bin ($i = 1, 2, 3, \dots, 20$). The time intervals were uniformly distributed with a bin width given by the formula $\Delta t^{(n)} = f^n$ ms, where f is a constant and n is the index of a histogram ($n = 0, 1, 2, 3, \dots$). Thus, for n -th histogram we obtained the following set of bins:
 $t_1 \leftrightarrow t_2 \leftrightarrow t_3 \leftrightarrow \dots \leftrightarrow t_{20}$
 $1 \text{ ms} \cdot f^n \leftrightarrow 2 \text{ ms} \cdot f^n \leftrightarrow 3 \text{ ms} \cdot f^n \leftrightarrow \dots \leftrightarrow 20 \text{ ms} \cdot f^n$

Table 1. Number of experiments under different conditions

Conditions	N_{channels}	N_{events}
250 mM KCl	11	4×10^5
500 mM KCl	6	1×10^6
750 mM KCl	8	1.8×10^8
1 M KCl	13	1×10^8
1.5 M KCl	10	1.3×10^8
2 M KCl	11	8×10^7
–40 mV	7	7.8×10^7
–20 mV	12	1.6×10^8
0 mV	13	1×10^8
+20 mV	10	9×10^8
+40 mV	14	2×10^8
+60 mV	14	6×10^7
+80 mV	9	2.2×10^7
+100 mV	3	3×10^3

N_{channels} , the number of single channel recordings used for kinetic analysis; N_{events} , the number of analyzed events (closings or openings).

Typically, we used $f = 1.1$ which gives the following set of histograms

$$\begin{aligned} n = 0: & 1 \text{ ms} \leftrightarrow 2 \text{ ms} \leftrightarrow 3 \text{ ms} \leftrightarrow \dots \leftrightarrow 20 \text{ ms} \\ n = 1: & 1.1 \text{ ms} \leftrightarrow 2.2 \text{ ms} \leftrightarrow 3.3 \text{ ms} \leftrightarrow \dots \leftrightarrow 22 \text{ ms} \\ n = 2: & 1.21 \text{ ms} \leftrightarrow 2.42 \text{ ms} \leftrightarrow 3.63 \text{ ms} \leftrightarrow \dots \leftrightarrow 24.2 \text{ ms} \end{aligned}$$

where n was kept growing as long as there was a reasonable distribution of time intervals in the first several bins (i.e. no empty bin in the first four bins (Liebovitch and Sullivan 1987)). For each histogram, obtained from a set of dwell times $N^{(n)}$, we determined a single exponential fit, from which we obtained the rate constant $k_{rate}^{(n)}$ typical for a the given time scale $\Delta t^{(n)} = f^n$. This approximates the dependence of the rate constant $k_{rate}(\Delta t)$ on the time scale used for histogram construction. In the following text, this rate constant is called effective rate constant, k_{eff} . Similarly, when we plot the discrete probability density (DPD) for every n :

$$DPD \equiv \frac{1}{\Delta t^{(n)} \sum_{i=1}^{20} N_i^{(n)}} \approx \rho(\Delta t) \quad (1)$$

and interpolate through all plots (all Δt used), we obtain the approximation for the probability density function (PDF): $\rho(\Delta t)$.

The dwell time histogram at each Δt was fitted with a simple exponential function:

$$N(\Delta t) = Ae^{-k(\Delta t)t} \quad (2)$$

where A is constant and $k(\Delta t)$ is the rate constant for each Δt . In the text, $k(\Delta t)$ is named the effective rate constant, k_{eff} .

The dependence of $k_{eff}(0)$ on Δt was fitted in Graph Pad Prism 9 by function ("log-log line, X and Y both log"):

$$k_{eff}(0) = 10^{S \cdot \log(\Delta t) + k_{intercept}} \quad (3)$$

where S is the slope of the line in the log-log plot.

Results

Description of the gating kinetics

The basic description of the mitochondrial chloride channel gating kinetics was determined in 1 M/50 mM KCl gradient at zero applied potential. In this gradient, the channels had a conductance of 204 ± 18 pS (mean, SD, $N = 5$). The

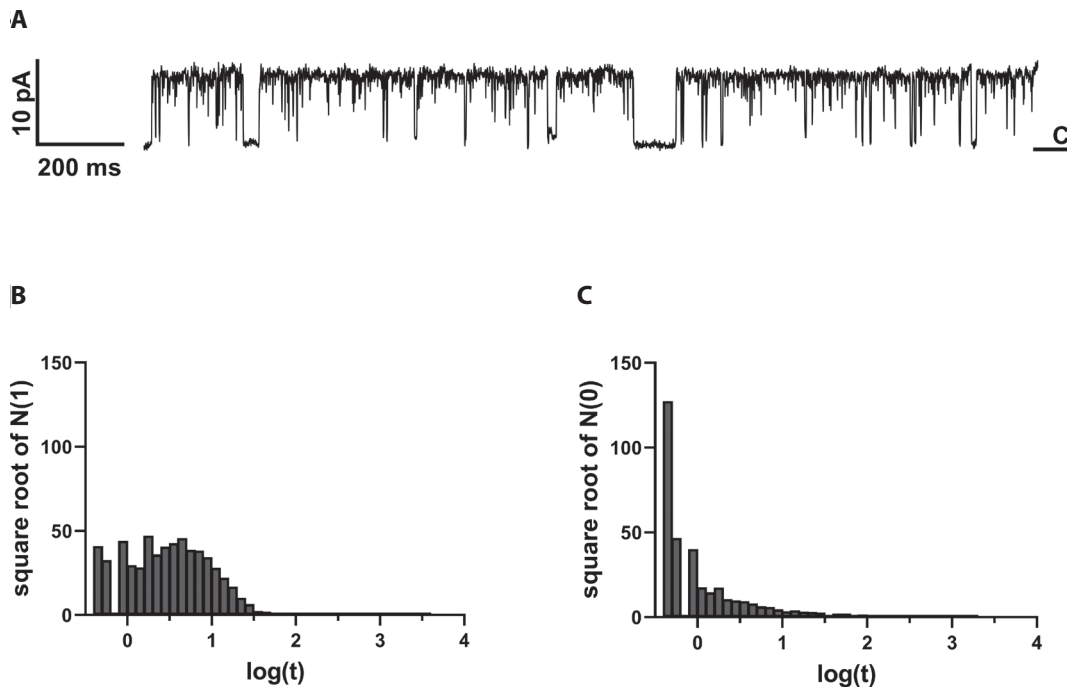


Figure 1. A. A typical current trace of a single channel, measured in 1 M/50 mM KCl gradient. Unresolved closings are frequently observed at 4 kHz sampling rate and 1 kHz filtering. "C" on the right side of the trace indicates closed level. B., C. Representative dwell time histograms from one single-channel recording. According to Sigworth and Sine (1987), Wonderlin et al. (1990), and Sakmann and Neher (2009), the presence of a peak(s) in the histogram with logarithmic time scale (10 bins *per* decade, time in ms) and square root of the number of events *per* bin correspond to the number(s) of kinetic state(s). Time t is in ms. The open dwell times (B) have a peak at approximately $10^{0.7}$ ms, which corresponds to a kinetic rate constant 200 Hz. On the other side, the closed dwell time lack any visible peak (C).

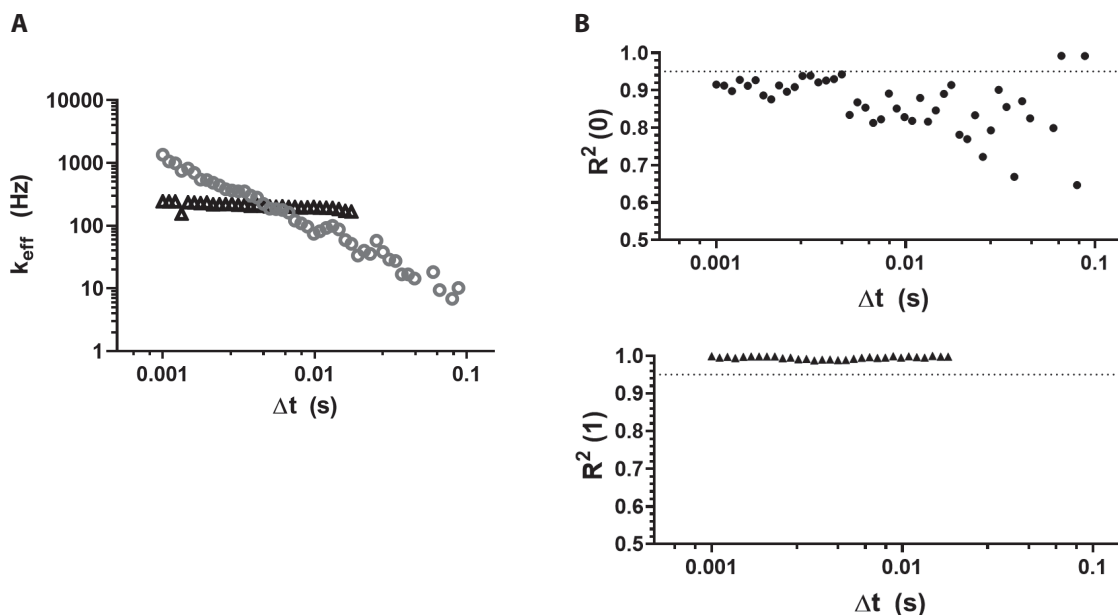


Figure 2. Effective rate constants from one single-channel recording measured at 1 M/50 mM KCl. **A.** Each circle or triangle represents a value of effective rate constant was obtained from exponential fit of dwell time histogram, having bin width equal to Δt . The effective rate constant for leaving the closed state, $k_{\text{eff}}(0)$, acquires values that depend on the bin width (grey circles), which is not the case of the $k_{\text{eff}}(1)$ for leaving the open state (black triangles). **B.** The values of R^2 at each Δt . The exponential function was well describing the open dwell times at all values of bin width (triangles), whereas for the closed dwell times, the quality of the fit was rather poor (circles). Dotted line represents $R^2 = 0.9500$.

representative dwell time histograms of closings and openings, visualized as square root of N on a logarithmic time scale, are shown in Figure 1. This type of display has been proposed as most suitable to visualize the kinetic states, which are presented as peak(s) in the histogram (Sigworth and Sine 1987). It is apparent from these histograms, that the open and the closed dwell times have different distributions. Contrary to the open dwell times that exhibit a clear peak, the closed dwell times do not have the pattern of exponential distribution.

We used both the conventional histograms and the logarithmic histograms with square root of event count (" \sqrt{N} vs. $\log t$ ") and fitted them using the corresponding predefined function in the Clampfit software ("*standard exponential*" and "*exponential log probability*", respectively; data not shown). For the open dwell times, both methods consistently yielded a single characteristic dwell time, corresponding to rate constant: 171 ± 18 Hz from the conventional histogram and 208 ± 28 Hz from the " \sqrt{N} vs. $\log t$ " histogram (mean, SEM, $N = 13$). On the other hand, the fitting of closed dwell time histograms resulted in a variable number of terms (from 2 to 5). The number of terms differed among both the individual channels and the histogram types of one channel.

Therefore, we applied the described approach to characterize the kinetics of closed events. We created a set of

dwell time histograms, each with a different bin width Δt . From these histograms, we determined the effective rate constants. Effective rate constants are expressed as a function of Δt (also called t_{eff} in Liebovitch et al. (1987)), that is the bin width (Fig. 2A). $k_{\text{eff}}(0)$ is the effective rate constant for leaving the closed state. The value of $k_{\text{eff}}(0)$ is strongly dependent on Δt used (Fig. 2A, grey circles). On the other hand, $k_{\text{eff}}(1)$ is the effective rate constant for leaving the open state. $k_{\text{eff}}(1)$ was approximately independent of Δt (Fig. 2A, black triangles). The corresponding values of the coefficient of determination R^2 for each exponential fit are depicted in Figure 2B.

The closed dwell times exhibit a small incidence of very long events. We describe the closed dwell times from the individual experiments and compare the results to the closed dwell times pooled together. The pooling would result in higher incidence of longer dwell times and, therefore, might lead to better description. We constructed a dwell time histogram of the pooled data from $N = 13$ single-channel recordings in 1 M/50 mM KCl gradient at 0 mV applied potential with the aim to create a probability density function. The dwell time histograms of the pooled data comprised approximately 10^8 values (number of events). We created the discrete probability density function, $\rho(\Delta t)$, from the dwell times according to Equation 1. Figure 3 shows $\rho(\Delta t)$ for 1 M $[\text{KCl}]_{\text{cis}}$ at 0 mV. The open dwell times distribu-

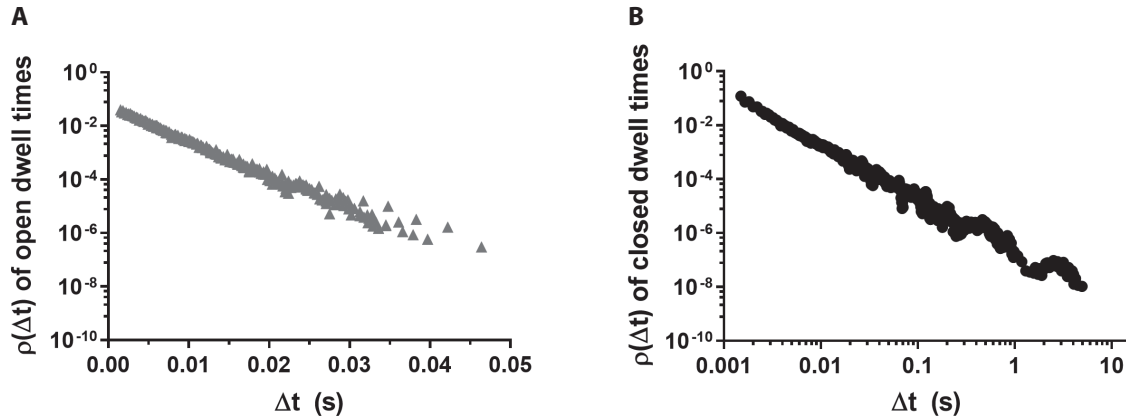


Figure 3. Difference between open and closed dwell time distribution. **A.** Probability density function of open dwell times is linear in semi-log plot, which is a property of exponential distribution. **B.** Probability density function of closed dwell times is linear in log-log plot, which corresponds to power-law distribution.

tion is linear in semi-log plot, which is consistent with the exponential distribution (Fig. 3A, triangles). On the other hand, $\rho(\Delta t)$ of closed dwell times is linear in the log-log plot (Fig. 3B, circles), which is a feature of the power-law distribution.

The value of $k_{\text{eff}}(1)$ from each experiment was determined as the arithmetic mean from the exponential fit at each Δt for every channel recording. The median and (Q_1 – Q_3) of the effective rate constant for the open state from $N = 13$ experiments was 141 (97–207) Hz. For comparison, we also pooled the open dwell times, from which a single $k_{\text{eff}}(1) = 128$ Hz was determined. This value is well within the range obtained from the individual experiments.

The values of $k_{\text{eff}}(0)$ as a function of Δt from the individual experiments were overlaid when plotted in one graph (Fig. S1

in Supplementary materials). The effective rate constants covering three orders of magnitude (0.8–1300 Hz) were detected consistently within each experiment, in some experiments the rate constants spanned four orders of magnitude (10^{-1} – 10^3 Hz).

To characterize the set of $k_{\text{eff}}(0)$, we determined one parameter: the slope of the dependence of $k_{\text{eff}}(0)$ on Δt from the log-log plot according to Equation 3. We compared the results from pooled data to averages from individual experiments. The mean value of the slope from individual experiments was -1.079 ± 0.096 (SD, $N = 13$). The fit from the pooled data yielded slope -1.101 with a 95% confidence interval from -1.132 to -1.072 ($R^2 = 0.9956$).

Concentration dependence of activity

The concentration dependence was measured in fixed KCl concentration in *trans* partition; the concentration was changed only in the *cis* partition from 0.25 to 2 M KCl. The activity, given by P_{open} , rises with increasing concentration of KCl in the *cis* compartment ($[\text{KCl}]_{\text{cis}}$). Corresponding single channel traces can be found in Figure S2. The dependence of the median P_{open} on $[\text{KCl}]_{\text{cis}}$ has sigmoidal character (Fig. 4); it was fitted using the Hill equation in the following form:

$$P_{\text{open}} = P_{\text{bottom}} + \frac{P_{\text{top}} - P_{\text{bottom}}}{1 + 10^{(\log EC_{50} - [\text{KCl}]_{\text{cis}}) \cdot n_{\text{Hill}}}} \quad (4)$$

where P_{bottom} and P_{top} are the plateaus of the activity, EC_{50} is the concentration at which the activity is half way between P_{bottom} and P_{top} ; n_{Hill} is the Hill slope. The fit, with $R^2 = 0.9984$, yielded best-fit values with standard error: $\log EC_{50} = -0.1106 \pm 0.007225$, which corresponds to $EC_{50} = 0.775$ M and $n_{\text{Hill}} = 8.173 \pm 1.242$. The Hill slope indicates the level of cooperativity among ligand binding sites (Weiss

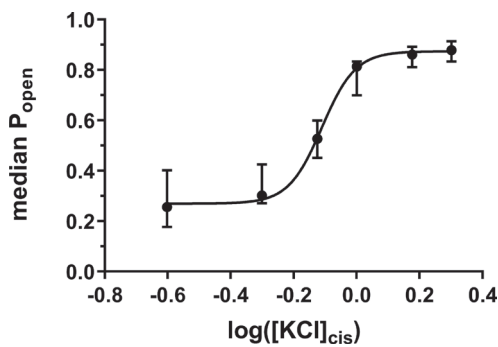


Figure 4. Concentration dependence of single channel activity. The channel activity expressed as median open probability P_{open} . The dependence has typical sigmoidal shape. Each point represents a median value obtained from all recordings at a given concentration. The median P_{open} values were fitted by Hill equation (line, Equation 4).

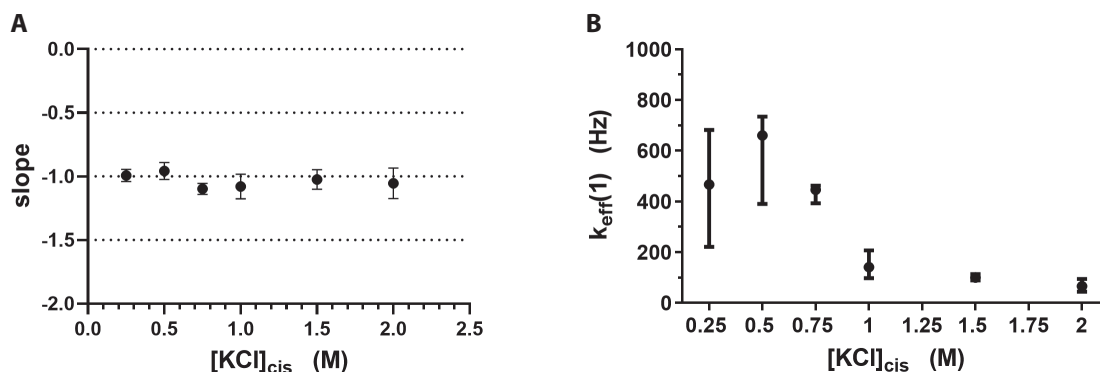


Figure 5. Concentration dependence rate constants. **A.** As it was impossible to determine one or a small number of effective rate constants for leaving the closed state, describe the set of $k_{\text{eff}}(0)$ by the slope of the dependence on Δt in log-log plot (obtained from Equation 3). The black circles represent mean slope values from individual experiments. **B.** The values of $k_{\text{eff}}(1)$ exhibited concentration dependence, which inversely followed the profile of P_{open} in Figure 4.

1997). In this case, we suppose the ligand is most likely the chloride anion.

Concentration dependence of gating kinetics

The values of $k_{\text{eff}}(0)$ span through four orders of magnitude from 0.1 to 1000 Hz. Interestingly, regardless of the $[\text{KCl}]_{\text{cis}}$ the property of $k_{\text{eff}}(0)$ to decrease monotonically with increasing Δt remains practically unchanged. We determined the slope of the dependence of $k_{\text{eff}}(0)$ on Δt from the log-log plot according to Equation 3. The slope values were determined from the individual experiments (Fig. 5A, black circles). We tested the difference between groups by one-way ANOVA ($p = 0.0096$). The following multiple comparison test showed significant differences between groups 0.5 M vs. 0.75 M KCl and 0.5 M vs. 1 M KCl. The mean slope values were also compared to the slope determined from the pooled closed dwell times (Figure S5A, grey squares).

The median value of $k_{\text{eff}}(1)$, obtained from the individual experiments, inversely follows the dependence of P_{open} on $[\text{KCl}]_{\text{cis}}$ (Fig. 5B); the abrupt shift in the values of $k_{\text{eff}}(1)$ near the inflection point is visible (between

0.75 M and 1 M). At 0.25 M and 0.5 M, the interval of $k_{\text{eff}}(1)$ is very broad, ~ 4 -times higher than at $[\text{KCl}]_{\text{cis}} \geq 0.75$ M. Nevertheless, the values of $k_{\text{eff}}(1)$ for each concentration are within one order of magnitude. The differences between groups were statistically significant ($p < 0.0001$, Kruskal-Wallis). There is a strong correlation between P_{open} and $k_{\text{eff}}(1)$, which is quantified by the Spearman coefficient $r = -0.9057$ (95% confidence interval from -0.9442 to -0.8428), two-tailed $p < 0.0001$, which is significant at $\alpha = 0.05$.

Voltage dependence of activity

The voltage dependence was measured in a fixed gradient 1 M/0.05 M KCl. The applied voltage was in the range from -40 mV to $+100$ mV. Lower voltages could not be used because the membranes were prone to breaking at less than -60 mV, thus, we could not measure the current below reversal potential of the channel in this gradient. The P_{open} of the channel has a bell-shaped dependence on voltage (Fig. 6), with maximum activity $P_{\text{open,max}} = 0.878$ (0.721–0.949), $N = 12$, achieved at $+20$ mV. At $+100$ mV, the activity of the

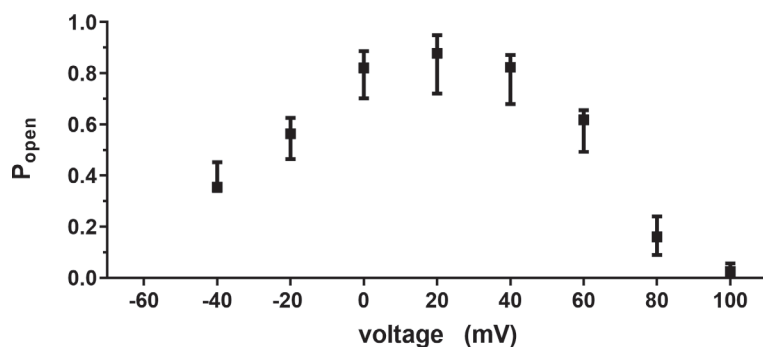


Figure 6. Voltage dependence of channel activity. The channel activity (P_{open}), measured in 1 M/50 mM KCl gradient, exhibits bell-shaped dependence on voltage. The artificial membranes were easily broken by voltages below -40 mV as well as by high positive voltages. The values of P_{open} are expressed as median and (Q_1 – Q_3).

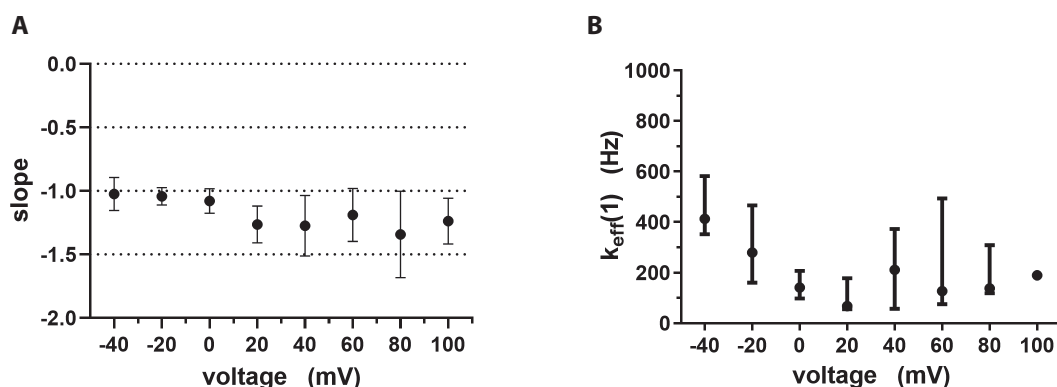


Figure 7. Voltage dependence of rate constants. **A.** The slope of the dependence of $k_{\text{eff}}(0)$ on Δt determined from log-log plot according to Equation 3. The black circles represent mean slope values from individual experiments. Multiple comparison test detected significant difference between -40 vs. $+80$ mV and -20 vs. $+80$ mV groups. **B.** Voltage dependence of $k_{\text{eff}}(1)$ values, expressed as median and (Q_1-Q_3) . The values of $k_{\text{eff}}(1)$ approximately inversely follows the profile of activity under different voltages.

channel was very rare and could be restored immediately by return to zero applied potential. We successfully measured only $N = 3$ channels at $+100$ mV.

Voltage dependence of gating kinetics

The voltage dependence was studied in a range from -40 mV to $+100$ mV, with increment of 20 mV. Corresponding single channel traces can be found in Figure S3. The character of closed dwell times distribution was unaltered upon voltage application: $\rho(\Delta t)$ of closed dwell times was linear in log-log scale, i.e. it has the power-law distribution. The spectrum of $k_{\text{eff}}(0)$ was similar to the concentration dependence, it ranged from 0.25 Hz to 1500 Hz. Again, the sets of $k_{\text{eff}}(0)$ are characterized by the slope of $k_{\text{eff}}(0)$ dependence on Δt in the log-log plot. The mean slope values are summarized in Figure 7A (black circles). One-way ANOVA indicated significant differences among groups ($p = 0.002$). The following multiple comparison test showed significant differences only between groups -40 mV vs. $+80$ mV and -20 mV vs. $+80$ mV. The mean slope values were also compared to the slope determined from the pooled closed dwell times (Fig. S5B, grey squares).

$r(\Delta t)$ of open dwell times also retained the exponential character, similarly to the concentration dependence. The range of $k_{\text{eff}}(1)$ values obtained from the separate experiments were comprised within two to three orders of magnitude. A single value of $k_{\text{eff}}(1)$ was detectable in each experiment, but the scatter of $k_{\text{eff}}(1)$ between channels was broad. The dependence of P_{open} on voltage approximately inversely follows the changes of median $k_{\text{eff}}(1)$, as can be seen in Figure 7B. The Kruskal-Wallis test indicated statistical significance ($p = 0.0135$), the following multiple comparison test showed significance only between -40 vs. $+20$ mV groups. The correlation between P_{open} and median $k_{\text{eff}}(1)$ was found to be

weak but significant: Spearman $r = -0.7305$; two-tailed $p = 0.0039$, significance level $\alpha = 0.05$.

Gating events at high resolution

The chloride channel current, measured in 1 M/ 50 mM KCl gradient at 0 mV applied potential, was recorded at 5 -times higher acquisition rate and correspondingly higher low-pass filter to detect the many unresolved and very fast events observed under standard acquisition settings (4 kHz sampling frequency, 1 kHz filter). Again, the recommended “ \sqrt{N} vs. $\log t$ ” dwell time histograms were created to visualize the dwell time distribution (Fig. 8). The data recorded with higher frequency are denoted as “ 5 kHz”, according to the filter frequency, the data acquired at lower frequency are denoted as “ 1 kHz”. The histogram of the closed dwell times exhibited, in 2 of 5 channels, an indication of peak very close to the detection limit (in the second smallest bin). However, after taking into account the profiles of the histograms in Figure 1, it might as well be a random deviation, because the counts in the bins are not evenly distributed. A single peak was observed in open dwell times histogram at $t \approx 10^0$ ms, which corresponds to 1 kHz gating frequency.

Interestingly, when we used the alternative approach to determine the values of k_{eff} at different bin widths, the character of these dependencies remained unchanged, except for the values of $k_{\text{eff}}(1)$. These were shifted to higher frequencies, as can be seen in Figure 9A. The median value of $k_{\text{eff}}(1)$ at 5 kHz filter and 20 kHz acquisition rate was 942 (604 – 1045) Hz, $N = 5$. The dependence of $k_{\text{eff}}(0)$ on bin width was linear in the log-log plot and yielded a mean slope value of -1.015 ± 0.063 ($N = 5$). The comparison of the $k_{\text{eff}}(1)$ values and the slopes describing $k_{\text{eff}}(0)$ dependence on bin width, obtained at different resolutions, is summarized in Figure 9.

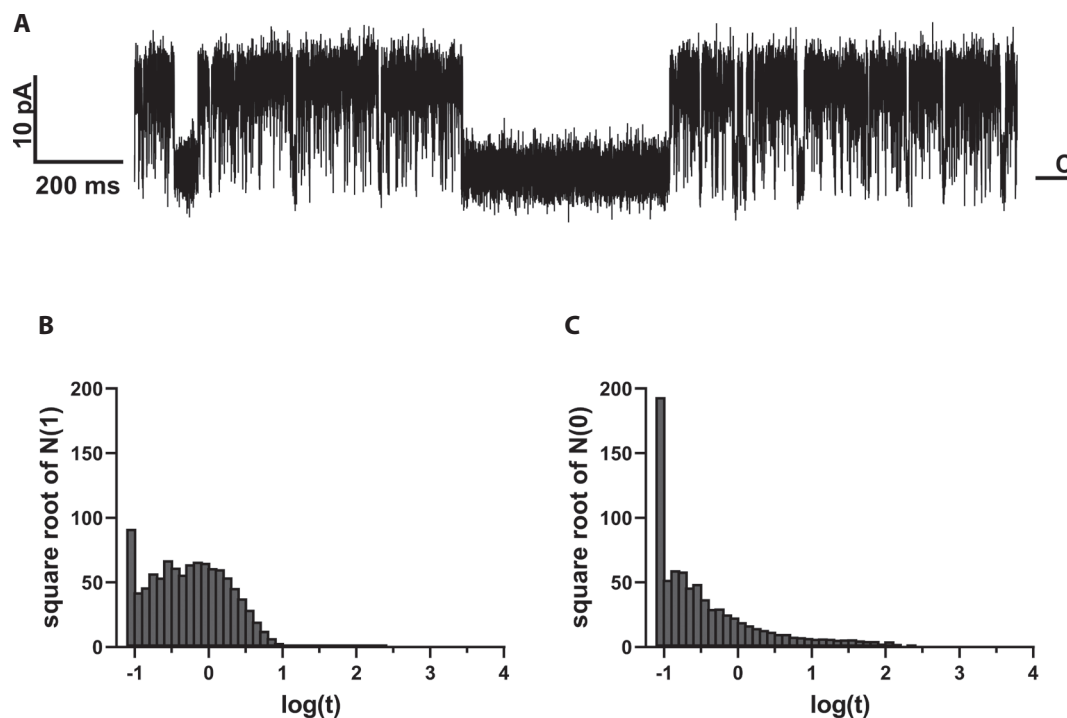


Figure 8. Current trace and distribution of dwell times at high resolution. **A.** Representative current trace acquired at 20 kHz sampling frequency and filtered at 5 kHz with low-pass filter. Even at the higher resolution, there are still closings that do not reach the baseline (unresolved closings). “C” depicts the closed level; the channel opens upward. **B.** The histogram open dwell times, with transformed axes, looks similar to the one shown in Figure 1, but the peak is shifted towards lower time values. **C.** Histogram of closed dwell times does not exhibit any marked peak. It is possible that the true closings are either much faster than the resolution available or are governed by a different mechanism with non-exponential distribution.

Discussion

While the chloride channels from cardiac mitochondrial membranes remain unknown on the genetic level, there are indications that these channels might be identical to CLIC5 isoform of the CLIC channel family (Misak et al. 2013; Ponnalagu et al. 2016). We describe a kinetic prop-

erty that could serve as another identifier of the native mitochondrial chloride channels. It could be helpful in a more detailed comparison with the recombinant CLIC5 channels or other chloride/anion channels (Kinnally et al. 1993; Tonini et al. 2000; Drummond-Main and Rho 2018). We analyzed the gating kinetics of the native channels under different conditions (voltage, concentration gradient).

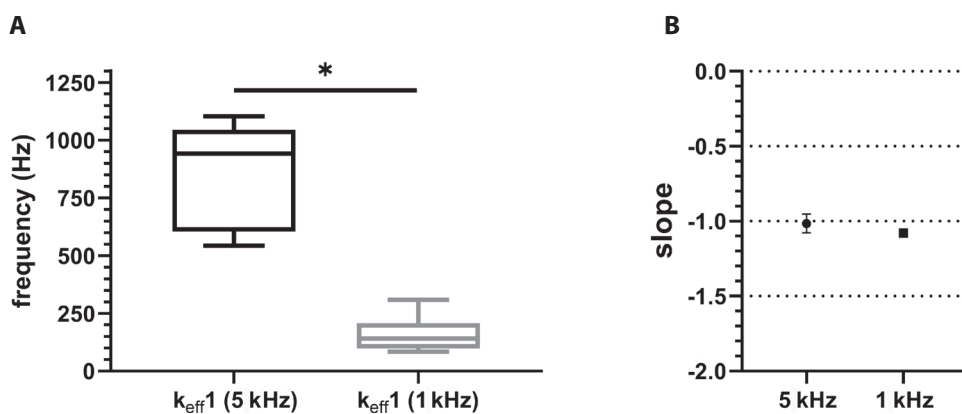


Figure 9. Comparison of kinetic parameters at different resolution. **A.** The median value of $k_{\text{eff}}(1)$ increased significantly (Mann-Whitney test, * $p = 0.0002$), when the channel current was recorded at 20 kHz and filtered at 5 kHz. **B.** The slope values describing the $k_{\text{eff}}(0)$ dependence on bin width were not changed when the channel current was recorded at higher acquisition rate (unpaired t-test, $p = 0.2791$).

As was observed previously, while studying the effects of a chloride channel inhibitor (Tomaskova et al. 2007), these channels exhibit bursts of activity and very fast unresolved closing events (Tomasek et al. 2017). The classic display of dwell time histogram indicated that the closed dwell times could not be described by an exponential function (Fig. 1). The comparison of conventional histograms and logarithmic “ \sqrt{N} vs. $\log t$ ” histograms yielded consistently a single characteristic dwell time for the open dwell times. On the other hand, the fitting of closed dwell time histograms resulted in a variable number of terms, differing both among individual channels and between the histogram types of one channel. Therefore, we looked for a different way to describe the kinetics of channel closings. Channels exhibiting similar kinetic features (bursts or very fast kinetics) were observed in Magleby and Pallotta (1983), Blatz and Magleby (1986), Ring (1986) and analyzed by the fractal model (Liebovitch et al. 2001). We partially used the analytical approach of the fractal model but we did not use the interpretation given by this model.

We constructed a set of histograms for each set of dwell times derived from single channel recording. These histograms differed in bin widths Δt , which increased according to the $\Delta t^{(n)} = 1.1$ ms relationship. Each histogram was fitted with single an exponential function and a rate constant was determined from each one. The effective rate constant $k_{\text{eff}}(1)$ for leaving the open state was approximately constant, insensitive to the bin width used for the underlying histogram. This was, however, not the case for inverse transitions, i.e. for leaving the closed state. It is, therefore, not possible to reliably determine a set of rate constants for leaving the closed state, $k_{\text{eff}}(0)$.

It is notable that the dwell-time histograms were fitted with a single-exponential function at each bin width, that is, a simple Markov model was used for each bin width. Usually when fitting dwell-time histograms, the bin width is optimized for each data set. Generally, it is different for each channel recording and also depends on the number of events in the recording. In case of the mitochondrial chloride channels, this does not present a problem for the analysis of the open dwell times. The closed dwell times, however, were characterized by different rate constant at each value of the bin width. This type of observation has been interpreted as the fractal behavior of the ion channels (Liebovitch et al. 2001). Two different explanations for this behavior exist: either the kinetic constant is changing in time or the protein has a broad spectrum of kinetic rate constants, each one corresponding to different conformation. Even though the author of this model states that the ‘multiscale’ method is capable of accurately characterizing both fractal and non-fractal probability density functions (Liebovitch et al. 2001), it is not generally accepted and several arguments have been raised against it, mostly against the interpretation

of the results. The most resonant objection was that even if the protein can have almost an infinite number of different conformations, only those that are relevant for ion transition should be taken into account. It has been shown that the Markov stochastic model fits the data better than the fractal model (McManus et al. 1988; Sakmann and Neher 2009). Furthermore, the use of fractal dimension does not have a physical meaning in terms of ion channel (Sakmann and Neher 2009).

Already in 1988, Lauser indicated that the fractal notion is not needed in the interpretation of non-exponentially distributed dwell times (Lauser 1988). Many channels exhibit such distribution of closed dwell times (Trautmann 1982; Magleby and Pallotta 1983; Horn and Vandenberg 1984; Sakmann and Trube 1984; Horn 1987; McGee Jr. et al. 1988). The non-exponential character is reflected in the increased occurrence of longer closed dwell times than predicted by the exponential function. Lauser presented a microscopic model of channel gating, based on small-scale motions within the protein, which was able to reproduce the experimentally detected dwell time distributions (Lauser 1988).

An alternative explanation of the non-exponential or multi-exponential dwell time distribution was proposed by Millhauser et al. (1988). The channel kinetics was described as Markov process but the resulting dwell time distribution had a power-law character. The physical interpretation was that the channel protein had a large number of conformational states with similar energies. The changes in the protein conformation were viewed as a diffusion process. The power-law distribution can be seen in desensitization of the acetylcholine receptor or inactivated voltage-gated channels (Millhauser et al. 1988). Often, higher number of exponentials is necessary to describe such a distribution; typically, the dwell times span through several orders of magnitude. The use of exponential functions is, however, mathematically incorrect for description of power-law distribution.

In the present study, we describe the power-law distribution of the closed dwell times of the cardiac mitochondrial chloride channels (Figs. 2 and 3). As we could not describe the distribution with a multiexponential function, the set of $k_{\text{eff}}(0)$ under different conditions was quantified by one parameter: slope of the dependence of $k_{\text{eff}}(0)$ on Δt , determined from log-log plot according to Equation 3. Based on the correlation of activity (P_{open}) and the rate constant $k_{\text{eff}}(1)$ and on the dependence of $k_{\text{eff}}(1)$ on the [KCl] gradient, it seems that the resulting activity is given by the changing rate constant for leaving the open state. The set of $k_{\text{eff}}(0)$ values was almost insensitive to the [KCl] gradient. Thus, it seems that the channel activity changes mainly through changes of the open state duration differences (Fig. 5).

The fit of P_{open} as a function of $[\text{KCl}]_{\text{cis}}$ using the Hill equation indicates that either the K^+ or the Cl^- serve as a ligand for the chloride channel (Fig. 4). The ligand activates

the channel in a cooperative way. According to Weiss (1997), the interpretation of the Hill coefficient is that it represents a minimum of binding sites for the given ligand. In the context of this interpretation, there are at least 8 binding sites for the ligand ion. Using the hypothesis presented in (Tomasek et al. 2017), there would be at least two binding sites on one conducting unit of the channel.

The activity of the channels was affected by the applied voltage, giving a bell-shaped profile of activity (Fig. 6). The maximal activity was achieved at approximately +20 mV (in 1 M/50 mM KCl). Similar voltage dependence of the mitochondrial chloride channels was described in different gradients (250/50 mM and 150/150 mM KCl) and it retained the bell-shaped profile centered around +20 mV (Tomaskova et al. 2007). Interestingly, the magnitude of the gradient did not affect the center of the voltage dependence profile, only its width. We observed that the voltage had a very small effect on the kinetics of closing. Although the slope values of the dependence of $k_{\text{eff}}(0)$ on Δt determined from the log-log plot were significant between some groups (Fig. 7), we did not observe any systematic shift in the values. At the positive voltages there was also a higher variance of the slope values. On the other hand, the median rate constants $k_{\text{eff}}(1)$ at different voltages differed significantly only between -40 mV and +20 mV. We observed the profile of $k_{\text{eff}}(1)$ on voltage depicted in Figure 7B also within one channel recording, with an applied voltage range from -40 to +80 mV (Figure S4). It approximately inversely follows the profile of channel activity, but the weak correlation between $k_{\text{eff}}(1)$ and P_{open} indicates that the resulting activity is not given only by the changes of open dwell times. It could be explained by the extremely long closings at higher voltages, which significantly lower the activity, but their occurrence is rare (e.g. 5 long closings, covering in sum 50 s, during one minute of recording; $P_{\text{open}} = 0.237$, number of events 2×10^3). Such a low number of long events does not contribute significantly to the distribution, nevertheless, it has a significant impact on the channel activity. The pooling of the closed dwell times did not give any further information in comparison to the averaged parameters from the individual experiments (Figure S5). The rare, extremely long dwell times did not contribute visibly to the profile of $k_{\text{eff}}(0)$ in the pooled data.

The current was recorded at a higher acquisition rate in order to better detect the fast closings of the channels (Figs. 8 and 9). It was reflected in an increased rate constant for channel openings, but the distribution of the closed dwell times remained unchanged. Noteworthy, the counts are several times higher in the smallest bin than in the following, second smallest bin. This high count in the smallest bin was not observed for open states at 1 kHz filter and 4 kHz sampling rate. It was present for 5 kHz open dwell times (Fig. 8B), which possibly comes from the increased noise/

unresolved events. It is present in the histogram of closed dwell times detected at both sampling rates.

Several questions arise from the described observations. Could it only be a tail of the dwell time histograms and the true closing frequency lies beyond the resolution, even at the 20 kHz acquisition rate? The Markov model is generally accepted and fitting of the histograms with an exponential function or a sum of exponential functions is widely used to determine channel kinetics. The usual concept is to fit the distribution that is visualized on non-transformed, linear axes (i.e. counts on ordinary axis and linear bins on abscissa axis). But is it correct to fit the untransformed histograms “blindly” with sum of the exponential functions, if the majority of events could not be detected? What is then the information obtained from the fit?

We were unable to determine the rate constant(s) for the channel closing. We tried to use a different analytical approach, which is not commonly used. From this, we described the determined set of rate constants for the closed state by the slope value. If the slope remains close to -1 under all tested conditions and even in case of the 20 kHz acquisition rate, is it not due to lack of a typical dwell time (rate constant)? Or is it an artefact, which originates from the unresolved events? The inexistence of a characteristic rate constant is compatible with the power-law distribution. When the protein switches to a closed state, it acquires a different conformation. This conformation changes in time and the longer the channel resides in the closed state, the higher is the energy required for switching back to the open state (Blatz and Magleby 1986; Millhauser et al. 1988; Liebovitch et al. 2001). The variations in structure (conformations) have been described in globular proteins – the energy profile of such structure consisted of many local minima (local energy barriers) and was not describable by the Markovian model (Karplus and McCammon 1981; Elber and Karplus 1987; Shen et al. 2001; Bandeira et al. 2008). Non-Markovian kinetics has been described for several ion channels (Liebovitch 1989) – voltage dependent potassium channels of different origin (Liebovitch and Sullivan 1987; Kazachenko et al. 2001), calcium-activated potassium channels (French and Stockbridge 1988; Bandeira et al. 2008) or gramicidin A channel (Ring 1986). Similar kinetics has been described in chloride channels from skeletal muscle (Blatz and Magleby 1986), but has been associated with non-Markovian kinetics only later (Liebovitch et al. 2001).

Concerning the invariability of the slopes in a log-log plot, we can look on the slope in the context of the fractal analysis. It linearly reflects the fractal dimension D . Similar, voltage-independent, D value ($D \sim 2$) was reported for voltage-dependent potassium channels and chloride channels from skeletal muscle (Liebovitch and Sullivan 1987). If the reader is interested in the interpretation of D , answers

can be found in the literature (Liebovitch et al. 1987, 2001; Liebovitch 1989).

On the other hand, if we stick to the Markov model, then the only explanation of the observed closed dwell time histograms (Fig. 1C) is that the true kinetic constant is so small, that we detect only the tail of the histogram even at the 20 kHz sampling rate. In such case, it is not appropriate to fit the histograms with exponential function and the detection of the true rate constant is beyond the limits of actual measurement devices.

We are rather inclined to the explanation that the mitochondrial chloride channels are of the power-law closed dwell time distribution, which has also been described in other ion channels and is consistent with the observations from molecular dynamics of other proteins.

Overall, the gating kinetics is a property resulting from the physical structure and set of possible conformations of a channel protein. It can therefore be used for comparison of the channels. There are channels, like the cystic fibrosis transmembrane conductance regulator (CFTR) channel (Schultz et al. 1995), voltage-dependent anion channel (VDAC) (Colombini 1989; Wunder and Colombini 1991; Sabirov and Merzlyak 2012) or the double-barreled chloride (CLC) channels (Miller 2006), that have visibly distinct kinetics. Nevertheless, there are several channels whose current traces are very similar to the channels we describe here – they have fast kinetics and occasional long closings (not always described as bursts). Their kinetics is usually characterized by simple dwell time histograms, not the “ \sqrt{N} vs. $\log t$ ” histogram. Moreover, they are mostly of unknown molecular origin as well (Klitsch and Siemen 1991; Kinnally et al. 1992, 1993; Dulhunty et al. 1996; Kourie 1997; Tonini et al. 2000; Singh and Ashley 2007; Drummond-Main and Rho 2018). However, the most interesting is the similarity to CLIC channels described in Tonini et al. (2000) and Singh and Ashley (2007), because the CLIC isoforms have been detected in the mitochondrial membrane (Ponnalagu et al. 2016). Previously, we have reported other properties that indicate similarity of the cardiac mitochondrial chloride channels to the CLIC (Misak et al. 2013; Tomasek et al. 2017).

The chloride channels derived from cardiac mitochondrial membranes exhibited the closed dwell time distribution that could not be reliably described by a sum of exponential functions. It would be intriguing to find a channel that is of similar distribution of closed dwell times and at the same time its crystallographic structure is known, along with molecular dynamics simulations. This kind of information is available for some potassium channels (Sansom et al. 2002; DeMarco et al. 2019; Catacuzzeno et al. 2020; Fagnen et al. 2020). With ever progressing computing capacity, it might lead to understanding of the underlying mechanism that either provides non-exponential distribu-

tion or allows such fast closings that they cannot be detected using standard devices. Nevertheless, for comparison of the kinetics at the most basic experimental level, it requires simply displaying the data on a square root vs. logarithm scale, as was recommended in Sakmann and Neher (2009) or Wonderlin et al. (1990), which is, unfortunately, often not done.

Conclusion

The character of the dwell times distribution is an intrinsic property of the channel protein. It can be used as the channel's identity. We found that the open dwell times can be described by a simple exponential function, but the closed dwell times do not follow the exponential distribution. The character of the distributions was retained under different voltages and concentration gradients. The changes in channel activity due to a different KCl gradient were reflected in the change of the open dwell time distribution. The applied voltage affected distribution of open dwell times, which approximately inversely followed the P_{open} profile. The distribution of closed dwell times was almost unaffected by the conditions used and remained the same even at a higher acquisition rate. Its distribution was consistent with the power-law distribution.

Conflicts of interest. The authors have no conflict of interest.

Acknowledgements. This work was supported by Scientific Grant Agency of MESRaS and SAS, namely grant VEGA 02/0090/18 and VEGA 02/0146/16. We thank the Slovak Centre of Scientific and Technical Information for free access to Matlab R2015a (<http://cvtisr.sk/>). The software for analysis in Matlab was developed by MT Research, <https://www.mitorex.net/>, Brezova pod Bradlom, Slovak Republic. The Clampfit software was kindly provided by Dr. Alexandra Zahradnikova. We thank Dr. Robert Sevcik for valuable discussions, and Dr. Tereza Golias, Dr. Katarina Polcicova and Dr. Peter Schlosser for language corrections.

References

- Aon MA, Cortassa S, Marbán E, O'Rourke B (2003): Synchronized whole cell oscillations in mitochondrial metabolism triggered by a local release of reactive oxygen species in cardiac myocytes. *J. Biol. Chem.* **278**, 44735-44744
<https://doi.org/10.1074/jbc.M302673200>
- Aon MA, Cortassa S, Akar FG, Brown DA, Zhou L, O'Rourke B (2009): From mitochondrial dynamics to arrhythmias. *Int. J. Biochem. Cell Biol.* **41**, 1940-1948
<https://doi.org/10.1016/j.biocel.2009.02.016>
- Bandeira HT, Barbosa CTE, De Oliveira RAC, Aguiar JF, Nogueira RA (2008): Chaotic model and memory in single calcium-activated potassium channel kinetics. *Chaos* **18**, 033136
<https://doi.org/10.1063/1.2944980>

- Blatz AL, Magleby KL (1986): Quantitative description of three modes of activity of fast chloride channels from rat skeletal muscle. *J. Physiol.* **378**, 141-174
<https://doi.org/10.1113/jphysiol.1986.sp016212>
- Catacuzzeno L, Sforza L, Franciolini F (2020): Voltage-dependent gating in K channels: experimental results and quantitative models. *Pflügers Arch.* **472**, 27-47
<https://doi.org/10.1007/s00424-019-02336-6>
- Colombini M (1989): Voltage gating in the mitochondrial channel, VDAC. *J. Membr. Biol.* **111**, 103-111
<https://doi.org/10.1007/BF01871775>
- Cortassa S, Aon MA, Winslow RL, O'Rourke B (2004): A mitochondrial oscillator dependent on reactive oxygen species. *Biophys. J.* **87**, 2060-2073
<https://doi.org/10.1529/biophysj.104.041749>
- DeMarco KR, Bekker S, Vorobyov I (2019): Challenges and advances in atomistic simulations of potassium and sodium ion channel gating and permeation. *J. Physiol. (London)* **597**, 679-698
<https://doi.org/10.1113/JP277088>
- Doyle DA (2004): Structural changes during ion channel gating. *Trends Neurosci.* **27**, 298-302
<https://doi.org/10.1016/j.tins.2004.04.004>
- Drummond-Main CD, Rho JM (2018): Electrophysiological characterization of a mitochondrial inner membrane chloride channel in rat brain. *FEBS Lett.* **592**, 1545-1553
<https://doi.org/10.1002/1873-3468.13042>
- Dulhunty AF, Junankar PR, Eager KR, Ahern GP, Laver DR (1996): Ion channels in the sarcoplasmic reticulum of striated muscle. *Acta Physiol. Scand.* **156**, 375-385
<https://doi.org/10.1046/j.1365-201X.1996.193000.x>
- Elber R, Karplus M (1987): Multiple conformational states of proteins – a molecular-dynamics analysis of myoglobin. *Science* **235**, 318-321
<https://doi.org/10.1126/science.3798113>
- Fagnen C, Bannwarth L, Oubella I, Forest E, De Zorzi R, de Araujo A, Mhoumadi Y, Bendahhou S, Perahia D, Venien-Bryan C (2020): New structural insights into Kir channel gating from molecular simulations, HDX-MS and functional studies. *Nat. Sci. Rep.* **10**, 8392
<https://doi.org/10.1038/s41598-020-65246-z>
- Flood E, Boiteux C, Lev B, Vorobyov I, Allen TW (2019): Atomistic simulations of membrane ion channel conduction, gating, and modulation. *Chem. Rev.* **119**, 7737-7832
<https://doi.org/10.1021/acs.chemrev.8b00630>
- French AS, Stockbridge LL (1988): Fractal and Markov behavior in ion channel kinetics. *Can. J. Physiol. Pharmacol.* **66**, 967-970
<https://doi.org/10.1139/y88-159>
- Hille B (1992): *Ionic Channels of Excitable Membranes*, 2nd Edition. Sinauer Associates, Sunderland, MA, United States
- Horn R (1987): Statistical methods for model discrimination. Applications to gating kinetics and permeation of the acetylcholine receptor channel. *Biophys. J.* **51**, 255-263
[https://doi.org/10.1016/S0006-3495\(87\)83331-3](https://doi.org/10.1016/S0006-3495(87)83331-3)
- Horn R, Vandenberg CA (1984): Statistical properties of single sodium channels. *J. Gen. Physiol.* **84**, 505-534
<https://doi.org/10.1085/jgp.84.4.505>
- Karplus M, McCammon JA (1981): The internal dynamics of globular-proteins. *CRC Crit. Rev. Biochem.* **9**, 293-349
<https://doi.org/10.3109/10409238109105437>
- Kazachenko NV, Kochetkov VK, Aslanidi VO, Grinevich AA (2001): Analysis of fractal ion channel gating kinetics – kinetic rates, energy-levels, and activation-energies. *Biofizika* **46**, 1062-1070
- Kinnally KW, Antonenko YN, Zorov DB (1992): Modulation of inner mitochondrial-membrane channel activity. *J. Bioenerg. Biomembr.* **24**, 99-110
<https://doi.org/10.1007/BF00769536>
- Kinnally KW, Zorov DB, Antonenko YN, Snyder SH, McEnery MW, Tedeschi H (1993): Mitochondrial benzodiazepine receptor linked to inner membrane ion channels by nanomolar actions of ligands. *Proc. Natl. Acad. Sci. USA* **90**, 1374-1378
<https://doi.org/10.1073/pnas.90.4.1374>
- Klitsch T, Siemen D (1991): Inner mitochondrial-membrane anion channel is present in brown adipocytes but is not identical with the uncoupling protein. *J. Membr. Biol.* **122**, 69-75
<https://doi.org/10.1007/BF01872740>
- Kourie JI (1997): ATP-sensitive voltage- and calcium-dependent chloride channels in sarcoplasmic reticulum vesicles from rabbit skeletal muscle. *J. Membr. Biol.* **157**, 39-51
<https://doi.org/10.1007/s002329900214>
- Läuger P (1988): Internal motions in proteins and gating kinetics of ionic channels. *Biophys. J.* **53**, 877-884
[https://doi.org/10.1016/S0006-3495\(88\)83168-0](https://doi.org/10.1016/S0006-3495(88)83168-0)
- Liebovitch LS, Sullivan JM (1987): Fractal analysis of a voltage-dependent potassium channel from cultured mouse hippocampal neurons. *Biophys. J.* **52**, 979-988
[https://doi.org/10.1016/S0006-3495\(87\)83290-3](https://doi.org/10.1016/S0006-3495(87)83290-3)
- Liebovitch LS, Fischbarg J, Koniarek JP, Todorova I, Wang M (1987): Fractal model of ion-channel kinetics. *Biochim. Biophys. Acta* **896**, 173-180
[https://doi.org/10.1016/0005-2736\(87\)90177-5](https://doi.org/10.1016/0005-2736(87)90177-5)
- Liebovitch LS (1989): Analysis of fractal ion channel gating kinetics – kinetic rates, energy-levels, and activation-energies. *Math. Biosci.* **93**, 97-115
[https://doi.org/10.1016/0025-5564\(89\)90015-1](https://doi.org/10.1016/0025-5564(89)90015-1)
- Liebovitch LS, Scheurle D, Rusek M, Zochowski M (2001): Fractal methods to analyze ion channel kinetics. *Methods* **24**, 359-375
<https://doi.org/10.1006/meth.2001.1206>
- Magleby KL, Pallotta BS (1983): Calcium dependence of open and shut interval distributions from calcium-activated potassium channels in cultured rat muscle. *J. Physiol.* **344**, 585-604
<https://doi.org/10.1113/jphysiol.1983.sp014957>
- McGee Jr R, Sansom MSP, Usherwood PNR (1988): Characterization of a delayed rectifier K⁺ channel in NG108-15 neuroblastoma X glioma cells: Gating kinetics and the effects of enrichment of membrane phospholipids with arachidonic acid. *J. Membr. Biol.* **102**, 21-34
<https://doi.org/10.1007/BF01875350>
- McManus OB, Weiss DS, Spivak CE, Blatz AL, Magleby KL (1988): Fractal models are inadequate for the kinetics of four different ion channels. *Biophys. J.* **54**, 859-870
[https://doi.org/10.1016/S0006-3495\(88\)83022-4](https://doi.org/10.1016/S0006-3495(88)83022-4)
- Mienville JM, Clay JR (1996): Effects of intracellular K⁺ and Rb⁺ on gating of embryonic rat telencephalon Ca²⁺-activated K⁺ channels. *Biophys. J.* **70**, 778-785
[https://doi.org/10.1016/S0006-3495\(96\)79617-0](https://doi.org/10.1016/S0006-3495(96)79617-0)

- Miller C (2006): CIC chloride channels viewed through a transporter lens. *Nature* **440**, 484-489
<https://doi.org/10.1038/nature04713>
- Millhauser GL, Salpeter EE, Oswald RE (1988): Diffusion models of ion-channel gating and the origin of power-law distributions from single-channel recording. *Proc. Natl. Acad. Sci. USA* **85**, 1503-1507
<https://doi.org/10.1073/pnas.85.5.1503>
- Misak A, Grman M, Malekova L, Novotova M, Markova J, Križanova O, Ondrias K, Tomaskova Z (2013): Mitochondrial chloride channels: Electrophysiological characterization and pH induction of channel pore dilation. *Eur. Biophys. J.* **42**, 709-720
<https://doi.org/10.1007/s00249-013-0920-2>
- Moss BL, Magleby KL (2001): Gating and conductance properties of BK channels are modulated by the S9-S10 tail domain of the alpha subunit. A study of mSlo1 and mSlo3 wild-type and chimeric channels. *J. Gen. Physiol.* **118**, 711-734
<https://doi.org/10.1085/jgp.118.6.711>
- Ponnalagu D, Gururaja Rao S, Farber J, Xin W, Hussain AT, Shah K, Tanda S, Berryman M, Edwards JC, Singh H (2016): Molecular identity of cardiac mitochondrial chloride intracellular channel proteins. *Mitochondrion* **27**, 6-14
<https://doi.org/10.1016/j.mito.2016.01.001>
- Reeves D, Ursell T, Sens P, Kondev J, Phillips R (2008): Membrane mechanics as a probe of ion-channel gating mechanisms. *Phys. Rev. E. Stat. Nonlin. Soft Matter Phys.* **78**, 041901
<https://doi.org/10.1103/PhysRevE.78.041901>
- Ring A (1986): Brief closures of gramicidin A channels in lipid bilayer membranes. *Biochim. Biophys. Acta* **856**, 646-653
[https://doi.org/10.1016/0005-2736\(86\)90160-4](https://doi.org/10.1016/0005-2736(86)90160-4)
- Sabirov RZ, Merzlyak PG (2012): Plasmalemmal VDAC controversies and maxi-anion channel puzzle. *Biochim. Biophys. Acta* **1818**, 1570-1580
<https://doi.org/10.1016/j.bbamem.2011.09.024>
- Sakmann B, Trube G (1984): Voltage-dependent inactivation of inward-rectifying single-channel currents in the guinea-pig heart cell membrane. *J. Physiol.* **347**, 659-683
<https://doi.org/10.1113/jphysiol.1984.sp015089>
- Sakmann B, Neher E (2009): *Single-Channel Recording*. 2nd edition, Springer-Verlag New York, NY, United States
- Sansom MSP (1995): Ion-channel gating – twist to open. *Curr. Biol.* **5**, 373-375
[https://doi.org/10.1016/S0960-9822\(95\)00076-5](https://doi.org/10.1016/S0960-9822(95)00076-5)
- Sansom MSP, Shrivastava IH, Bright JN, Tate J, Capener CE, Biggin PC (2002): Potassium channels: structures, models, simulations. *Biochim. Biophys. Acta* **1565**, 294-307
[https://doi.org/10.1016/S0005-2736\(02\)00576-X](https://doi.org/10.1016/S0005-2736(02)00576-X)
- Shen TY, Tai K, McCammon JA (2001): Statistical analysis of the fractal gating motions of the enzyme acetylcholinesterase. *Phys. Rev. E. Stat. Nonlin. Soft Matter Phys.* **63**, 033136
<https://doi.org/10.1103/PhysRevE.63.033136>
- Schultz BD, Venglarik CJ, Bridges RJ, Frizzell RA (1995): Regulation of cfr Cl⁻ channel gating by ADP and ATP analogs. *J. Gen. Physiol.* **105**, 329-361
<https://doi.org/10.1085/jgp.105.3.329>
- Sigworth FJ, Sine SM (1987): Data transformations for improved display and fitting of single-channel dwell time histograms. *Biophys. J.* **52**, 1047-1054
[https://doi.org/10.1016/S0006-3495\(87\)83298-8](https://doi.org/10.1016/S0006-3495(87)83298-8)
- Singh H, Ashley RH (2007): CLIC4 (p64H1) and its putative transmembrane domain form poorly selective, redox-regulated ion channels. *Mol. Membr. Biol.* **24**, 41-52
<https://doi.org/10.1080/09687860600927907>
- Sorum B, Torocsik B, Csanady L (2017): Asymmetry of movements in CFTR's two ATP sites during pore opening serves their distinct functions. *eLife* **6**, e29013
<https://doi.org/10.7554/eLife.29013.021>
- Tomasek M, Misak A, Grman M, Tomaskova Z (2017): Subconductance states of mitochondrial chloride channels: implication for functionally-coupled tetramers. *FEBS Lett.* **591**, 2251-2260
<https://doi.org/10.1002/1873-3468.12721>
- Tomaskova Z, Gaburjakova J, Brezova A, Gaburjakova M (2007): Inhibition of anion channels derived from mitochondrial membranes of the rat heart by stilbene disulfonate – DIDS. *J. Bioenerg. Biomembr.* **39**, 301-311
<https://doi.org/10.1007/s10863-007-9090-1>
- Tonini R, Ferroni A, Valenzuela SM, Warton K, Campbell TJ, Breit SN, Mazzanti M (2000): Functional characterization of the NCC27 nuclear protein in stable transfected CHO-K1 cells. *FASEB J.* **14**, 1171-1178
<https://doi.org/10.1096/fasebj.14.9.1171>
- Trautmann A (1982): Curare can open and block ionic channels associated with cholinergic receptors. *Nature* **298**, 272-275
<https://doi.org/10.1038/298272a0>
- Venglarik CJ, Singh AK, Wang RP, Bridges RJ (1993): Trinitrophenyl-ATP blocks colonic Cl⁻ channels in planar phospholipid bilayers. *J. Gen. Physiol.* **101**, 545-569
<https://doi.org/10.1085/jgp.101.4.545>
- Weiss JN (1997): The Hill equation revisited: Uses and misuses. *FASEB J.* **11**, 835-841
<https://doi.org/10.1096/fasebj.11.11.9285481>
- Wonderlin WF, French RJ, Arispe NJ (1990): Recording and analysis of currents from single ion channels. In: *Neurophysiological Techniques* (Eds. AA Boulton, GB Baker, CH Vanderwolf), pp. 35-142, Humana Press, Totowa, NJ, United States
<https://doi.org/10.1385/0-89603-160-8:35>
- Wright JM, Peoples RW, Weight FF (1996): Single-channel and whole-cell analysis of ethanol inhibition of NMDA-activated currents in cultured mouse cortical and hippocampal neurons. *Brain Res.* **738**, 249-256
[https://doi.org/10.1016/S0006-8993\(96\)00780-9](https://doi.org/10.1016/S0006-8993(96)00780-9)
- Wunder UR, Colombini M (1991): Patch clamping VDAC in liposomes containing whole mitochondrial-membranes. *J. Membr. Biol.* **123**, 83-91
<https://doi.org/10.1007/BF01993966>

Received: September 9, 2021

Final version accepted: December 26, 2021